Static dipole polarizability of small mixed sodium–lithium clusters

R. Antoine, D. Rayane, A. R. Allouche, M. Aubert-Frécon, E. Benichou, F. W. Dalby, Ph. Dugourd, M. Broyer, and C. Guet

Citation: The Journal of Chemical Physics **110**, 5568 (1999); doi: 10.1063/1.478455
View online: http://dx.doi.org/10.1063/1.478455
View Table of Contents: http://scitation.aip.org/content/aip/journal/jcp/110/12?ver=pdfcov
Published by the AIP Publishing

Static dipole polarizability of small mixed sodium–lithium clusters

R. Antoine, D. Rayane, A. R. Allouche, M. Aubert-Frécon,
E. Benichou, F. W. Dalby, Ph. Dugourd, and M. Broyer
Laboratoire de Spectrométrie Ionique et Moléculaire, Université Lyon I et CNRS, 43 Bd du 11 Novembre 1918, 69622 Villeurbanne Cedex, France

C. Guet
Département de Recherche Fondamentale sur la Matière Condensée, Service des Ions, des Atomes et des Agrégats, CEA Grenoble, 17 rue des Martyrs, 38054 Grenoble Cedex 9, France

(Received 3 August 1998; accepted 23 December 1998)

We have measured the static dipole polarizability of $Na_{y-x}Li_x$ clusters (with $y=2$, 3, 4, and 8) by molecular beam deflection technique. For a given size, the polarizability of pure lithium clusters is smaller than the polarizability of pure sodium clusters. For mixed clusters, a smooth decrease in the polarizability is observed as the proportion of lithium atoms increases. For the NaLi molecule, both experimental permanent dipole and average polarizability have been obtained. Experimental results are compared to results of density functional theory and configuration interaction single and double (CISD) *ab initio* calculations. © *1999 American Institute of Physics.* [S0021-9606(99)01512-3]

I. INTRODUCTION

Alkali clusters have been extensively studied both experimentally and theoretically. While lithium clusters and sodium clusters are both considered as simple models for metallic clusters, numerous works have underlined geometrical and electronic differences between these two systems. For a review, see for example Refs. 1–3. The study of mixed sodium–lithium clusters gives new insights to understanding the fundamental differences between these two simple systems. In a recent paper, we have reported an experimental and theoretical study of the ionization potentials of sodium–lithium clusters.[4] We focused on the geometrical differences between small sodium and small lithium clusters. In particular, we have shown that the substitution of a few sodium atoms by lithium atoms in sodium pentamers and hexamers induces a 2D to 3D transition.

In this article, we present a study of the static dipole polarizability of mixed sodium–lithium clusters. The static dipole polarizability is a direct test of the electronic properties of a molecule or a cluster in its ground state.[5,1] Sodium and lithium atoms have very close polarizabilities ($\alpha=23.6$ and $\alpha=24.3\,\text{Å}^3$, respectively).[6] Polarizabilities of sodium clusters were measured several years ago by Knight *et al.*[7] They change regularly from the atom to the bulk value. In fact, they roughly follow the classical evolution expected for a finite metallic sphere. Recently, we have reported the first measurements of lithium clusters' polarizability.[8] For small sizes, we observe a very sharp decrease in the polarizability per atom as the cluster size increases. While sodium and lithium atomic polarizabilities are almost equal, polarizabilities of Na_8 and Li_8 differ by more than 50%. Thus in this article we focus on the electronic properties of mixed sodium–lithium clusters made of only a few atoms.

Section II describes the experimental setup and the principle of the beam deflection technique. The theoretical approach is given in Sec. III. Results for diatomic molecules are given in Sec. IV, and the polarizability of small clusters is discussed in Sec. V.

II. EXPERIMENT

Figure 1 shows a schematic of the experimental setup. The polarizability measurements are made by deflecting a cluster beam through a static inhomogeneous transverse electric field $(F, dF/dz)$. Alkali clusters are produced in a seeded molecular beam. The heterogeneous alkali Na–Li clusters are generated by coexpansion of lithium–sodium vapor and 3–4 bars of argon through a 100 μm nozzle. Pure isotopically lithium and sodium rods are purchased from commercial sources. Sodium and lithium metals are heated at 1300–1350 K by two molybdenum ribbons which surround the cartridge. The collinear part of the beam is extracted through two 1 mm skimmers and tightly collimated by two 0.35 mm slits. The distance between the two slits is 1 m.

A. Deflection measurements

The collimated cluster beam goes through a 15 cm long deflector. The deflector is made of two cylindrical electrodes' faces which are 1.7 mm apart. The electrical field F between the two poles is equivalent to an ''electrical two-wire field.'' [9] This geometry provides both an electric field F and a field gradient dF/dz which are nearly constant over the width of the collimated cluster beam. A difference of potential of up to 30 kV can be applied between the two electrodes. This corresponds to an electric field of $1.8\ 10^7$ V/m and a gradient field of $3.2\ 10^9$ V/m^2. The interaction of the permanent dipole and of the induced dipole of the clusters with the nonuniform electric field deflects the clusters.

The deflection of a cluster is measured 1 m after the deflector in the extraction region of the first time of flight (TOF 1 in Fig. 1). The neutral clusters are ionized by a laser. Ions are then accelerated perpendicularly to the neutral beam

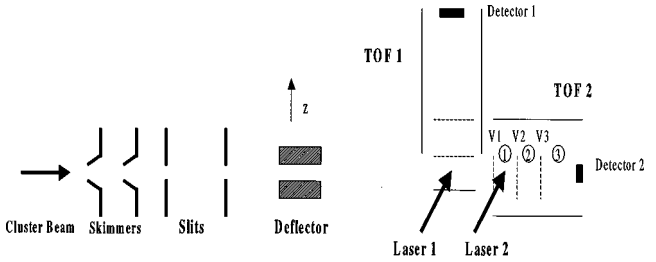

FIG. 1. Schematic of the experimental apparatus. The sensitive position time-of-flight mass spectrometer TOF 1, and the coaxial mass spectrometer TOF 2, are represented. TOF 1 is used for the deflection measurements, and TOF 2 is used for the velocity measurements. Regions 1, 2, and 3 represent, respectively, the extraction, acceleration, and field-free region of TOF 2.

and mass selected in the TOF mass spectrometer (TOF 1). The electric field in the extraction and acceleration region of the time of flight are adjusted so that the arrival time of a cluster at the detector is sensitive to the initial position of the cluster in the extraction region (position sensitive time-of-flight technique).[10,11] The deflection d of a cluster is determined by the comparison of its arrival time at the detector to the arrival time measured without electric field in the deflector. For the ionization, we used for clusters with $n \geqslant 3$ the fourth harmonic of a Nd:YAG ($\lambda = 266\,\text{nm}$, $\phi = 1\,\text{mJ/cm}^2$). Alkali molecules (Na_2, NaLi, and Li_2) are ionized by the resonant two-photon ionization (TPI) technique. This technique allows one to select a given vibronic and rotational state of the molecule. In the TPI technique, a first laser (dye laser) excites the A or B state of the dimers, and a second one [XeCl laser ($\lambda = 308\,\text{nm}$)] ionizes the excited molecules after an optical delay of a few nanoseconds.

The average polarizability of the clusters can be calculated from the deflection d, by Eq. (1),

$$\alpha = \frac{2dmv^2}{l(2L+l)F\dfrac{dF}{dz}}, \tag{1}$$

where l is the length of the deflector, L is the distance between the electrodes and the ionizing region, m and v are, respectively, the mass and the velocity of the clusters. z is the direction of the electrical field in the deflector. The main source of errors in the polarizability measurements is given by the precision of the velocity measurements. As discussed below, for atoms and dimers the precision for the velocity is 2%, and for clusters ($n \geqslant 3$), 5%. This leads to a precision for the polarizabilities of 4% and 10%, respectively.

B. Velocity measurements

Velocity measurements have been made with a TOF mass spectrometer mounted coaxially to the beam (TOF 2 in Fig. 1). For atoms and diatomic molecules we used an original technique which gives a precise value both for the mean velocity and for the width of the velocity distribution. Clusters are ionized between two plates in a free electrical field region (region 1, V1=V2=V). They fly 2 cm before entering region 2, where they are accelerated by the difference of potential V. Region 3 is a 30 cm long free electrical field region. The acceleration voltage V can be pulsed and delayed after the ionization laser pulse (laser 2, in Fig. 1). Figure 2(a) shows the signal observed for Na_2 with a constant voltage V (or a delay between the laser pulse and the voltage pulse inferior to $\Delta t = 9\ \mu$s). A flat broad peak is observed. The broadness of the peak is due to the spatial extension of the laser and to the width of the distribution of the initial velocity of the molecules. The peak observed with a delay of $\Delta t = 12\ \mu$s between the ionization laser pulse and the voltage pulse is much narrower. As seen in Fig. 2(a), with this delay, clusters have entered region 2 before the pulse is applied. The acceleration of a cluster depends on its position in the acceleration region. A refocalization of the ion pulse occurs. For a delay contained between $\Delta t = 10$ and $\Delta t = 12\ \mu$s, a part of the ion pulse is in region 1 and a part in region 2 while the voltage pulse is applied. A partial refocalization is observed [see Fig. 2(b)]. Only the distance between the laser position and the beginning of region 2 is needed to obtain a precise determination of the velocity of the molecules. For the spectra shown in Fig. 2, Na_2 molecules were generated under source conditions of 1100 K and 3.5 bars of argon. A sharp and symmetrical velocity distribution is observed. A mean velocity of 1270, with a dispersion of ± 50 m/s, is obtained, which is slightly greater than the estimated terminal velocity of argon from the thermodynamical properties of supersonic beams (around 1070 m/s).[12] The preci-

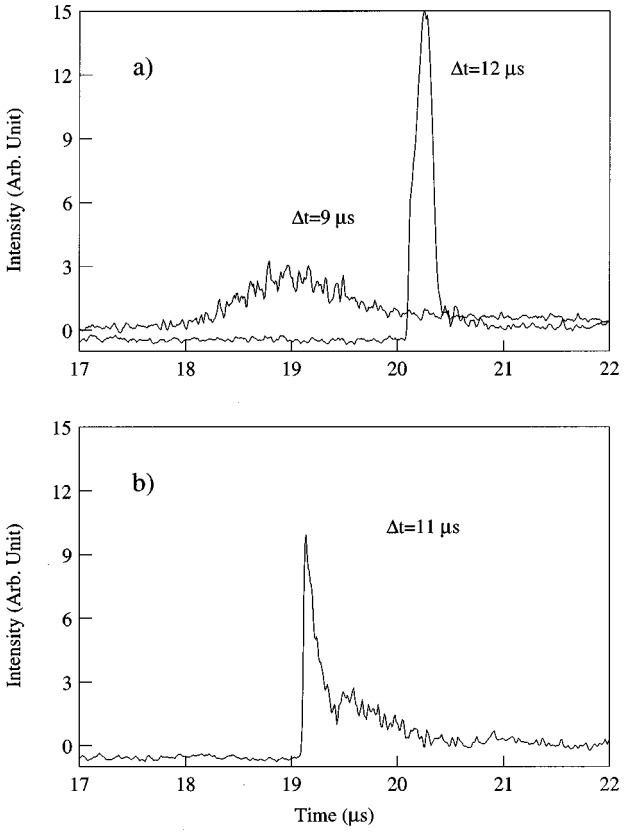

FIG. 2. Arrival time distributions (ATD's) of Na_2 molecules detected in the coaxial TOF mass spectrometer, with V1=V2=1000 V and with different time delays between the ionizing laser and the extraction voltage pulse [time delays of $\Delta t = 9$ and $\Delta t = 12\ \mu$s in Fig. 2(a) and $\Delta t = 11\ \mu$s in Fig. 2(b)].

sion on the mean velocity is 2%. Under these conditions, the mean velocities of Na, Li atoms, and Li_2 molecules are respectively 1260, 1390, and 1360 m/s.

The procedure described above can only be applied for atoms and diatomic molecules. For clusters, the peaks observed without refocalization are too broad to resolve the different sizes. For clusters, we applied an extraction and an acceleration voltage in region 1 and 2 (V1>V2). The arrival time on the detector depends on the initial kinetic energy of the clusters. Velocity is obtained by comparing experimental arrival time and calculated arrival time for a given initial kinetic energy. We used the velocity obtained for monomers and dimers with the method described above to carefully check the TOF parameters used for these simulations. The precision with this method is 5%. The velocities slowly decrease with the cluster size. (At 1100 K, for sodium, the velocity decreases from 1250 m/s for Na_3 to 1232 m/s for Na_{10}, and for lithium, the velocity decreases from 1328 m/s for Li_3 to 1307 m/s for Li_{10}). For identical source conditions, sodium cluster velocities are ≈5%–6% smaller than lithium cluster velocities. Thus, since velocities are very close (within the experimental error), we assumed a simple interpolation law to determine the velocity of heterogeneous NaLi clusters, i.e., $v_{\mathrm{Na}_n\mathrm{Li}_m}=v_{\mathrm{Na}_n}+m/n+m(v_{\mathrm{Li}_m}-v_{\mathrm{Na}_n})$.

III. THEORETICAL APPROACH

Gradient corrected density functional theory calculations, with Perdew–Wang 91 functional (DFT/PW91),[13] have been performed for all the cluster sizes investigated here. For atoms, dimers, and Li_3, configuration interaction calculations including single and double excitations (CISD) have also been performed at both valence-only electrons and all-electrons levels. For all these calculations, we used the Gaussian basis sets of Sadlej and Urban,[14] which have been specifically developed for polarizability calculations of alkali atoms. In particular, for the pure alkali clusters, this basis set gives a better agreement than the 6-31G basis set.[15]

The Cartesian components of the permanent dipole moment μ_i and of the static dipolar polarizabilities α_{ij} may be defined in terms of a Taylor expansion of the cluster energy E in an uniform electric field $\mathbf{F}$,

$$E(\mathbf{F})=E(\mathbf{0})-\sum_i \mu_i F_i-\frac{1}{2}\sum_{i,j}\alpha_{ij}F_iF_j+\cdots, \tag{2}$$

where $F_i(i\in\{x,y,z\})$ are the components of the field at the center of mass of the cluster. The components of the static dipole polarizability tensor can be obtained as the second derivatives of the energy with respect to the Cartesian components of the electric field,

$$\alpha_{ij}=-\left[\frac{\partial E}{\partial F_i \partial F_j}\right]_{F=0}. \tag{3}$$

In the DFT approach, the static polarizability components are obtained from the above equation. The second-order derivatives of the energy are computed analytically.[16]

In the CISD approach, the static dipole polarizability components were obtained numerically from Eq. (2) using a value of 10^{-4} (in a.u.) for the electric field F. The permanent dipole moment is obtained by evaluating the matrix element $\langle\psi|\mathbf{r}|\psi\rangle$, where ψ is the ground state CI wave function.

TABLE I. Interatomic distances (in Å), calculated static dipole polarizability per atom (in $Å^3$), along the principal axes (α_{ii}/n) and the corresponding average polarizability per atom (α_{moy}/n) for alkali atoms and diatomic molecules. The permanent dipole moment μ (in D) for the NaLi molecule is also given. Experimental values for the interatomic distances (in Å), and average polarizability per atom are given.

		R_e	$\alpha_{xx}(=\alpha_{yy})/n$	α_{zz}/n	α_{moy}/n	μ
Na	DFT/PW91		24.4	24.4	24.4	
	CISD(11*e*)		24.7	24.7	24.7	
	Exp.				23.6[a]	
Li	DFT/PW91		22.4	22.4	22.4	
	CISD(3*e*)		25.5	25.5	25.5	
	Exp.				24.3[a]	
Li_2	DFT/PW91	2.77	13.3	22.4	16.3	
	CISD(2*e*)	2.72	12.7	23.8	16.4	
	CISD(6*e*)	2.71	12.7	22.5	16.0	
	Exp.	2.67[b]			16.4	
NaLi	DFT/PW91	2.95	14.3	24.5	17.7	
	CISD(2*e*)	2.96	14.8	28.1	19.2	
	CISD(14*e*)	2.90	14.0	24.1	17.4	0.48[d]
	Exp.	2.89[c]			19.5	0.49
Na_2	DFT/PW91	3.11	15.2	26.6	19.0	
	CISD(2*e*)	3.20	17.3	32.9	22.5	
	CISD(22*e*)	3.09	15.4	26.7	19.2	
	Exp.	3.08[b]			20.0	

[a]Reference 6.
[b]Reference 19.
[c]Reference 20.
[d]Calculation performed with CISD (ten electrons).

DFT and CI polarizability calculations were performed using the package GAUSSIAN 94.[17] Dipole calculations were performed using the package MOLCAS.[18]

For atoms and dimers, DFT and CISD results for the polarizability diagonal tensor elements $\alpha_{xx}(=\alpha_{yy})$, α_{zz}, and the average polarizability $\alpha_{\mathrm{moy}}=1/3(\alpha_{xx}+\alpha_{yy}+\alpha_{zz})$ per atom, are given in Table I. For atoms, a good agreement between experimental $[\alpha(\mathrm{Na})=23.6\,Å^3,\ \alpha(\mathrm{Li})=24.3\,Å^3]$[6] and the all-electrons CISD calculated $[\alpha(\mathrm{Na})=24.7\,Å^3,\ \alpha(\mathrm{Li})=25.5\,Å^3]$ polarizabilities is obtained. For the sodium atom, the value obtained with the DFT/PW91 calculation $[\alpha(\mathrm{Na})=24.4\,Å^3]$ is also in very good agreement with the experimental value. For the lithium atom, the DFT/PW91 calculated value $[\alpha(\mathrm{Li})=22.4\,Å^3]$ slightly underestimates the experimental polarizability. For dimers, bond lengths were optimized for each calculation performed in the present work, i.e., DFT, CI-valence electrons, and CI-all electrons. The obtained values are in good agreement with experimental results (see Table I).[19,20] The static dipole polarizabilities calculated with the DFT/PW91 and with all-electrons CISD calculation are within 10% of the experimental values.

The DFT/PW91 approach was used to obtain polarizabilities of mixed alkali trimers and tetramers and small pure alkali octamers. For Li_3, CISD (three electrons and all-electrons) calculations have also been performed. Geometry optimization was performed with the DFT/PW91 calculation by gradient techniques. The optimization process started with initial configurations obtained from previous *ab initio* calculations for pure metal alkali clusters.[21,22] For mixed

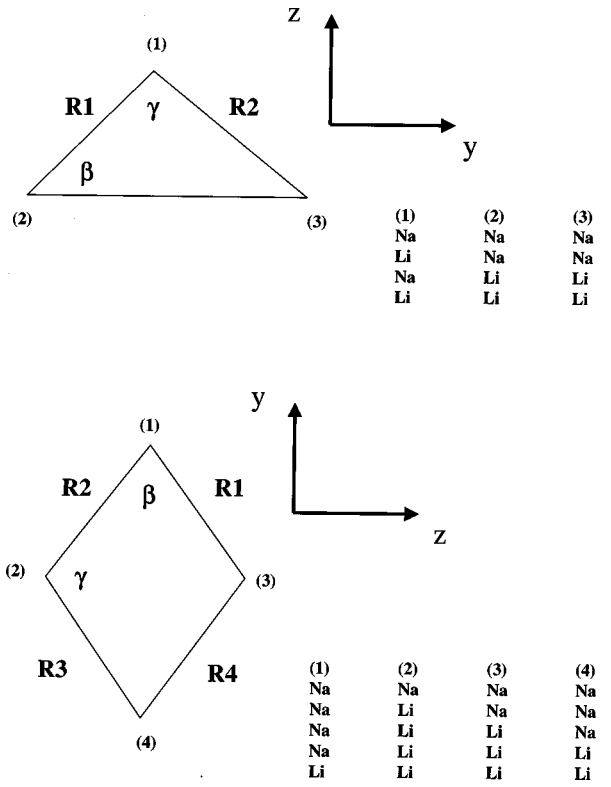

FIG. 3. Axis conventions and geometries for trimers and tetramers.

sodium–lithium clusters, we used as initial configurations, the geometries deduced from our recent theoretical investigation.[4] Figure 3 displays the conventions used for trimer and tetramer geometries and orientations. For each cluster, the polarizability tensor elements were calculated and the matrix was diagonalized, if necessary. Table II gives symmetry, interatomic distances, and angles for the ground state of the lowest-energy geometries obtained from our DFT/PW91 calculations. Ground-state geometries of sodium and lithium trimers are obtuse isosceles. For Li_3, optimized distances and angles are very close to experimental geometries.[2,23] The equilibrium conformation for Na_2Li is an isosceles triangle with an obtuse angle on the Li atom. $NaLi_2$ is found to be a triangle with a C_s symmetry and an acute angle on the sodium atom. Tetramers have rhombus planar geometries. In mixed tetramers, lithium atoms are preferentially located on the short diagonal of the rhombus. Our optimized structures on both trimers and tetramers are in good agreement with previous *ab initio* studies.[24–26] Ionization potentials (IPs) calculated for these structures are in close agreement with experimental values.[4] For the ground-state geometries of alkali octamers, we used, as initial configurations in the optimization process, the centered trigonal prism structure with a capped atom for Li_8, and the dicapped octahedral (dodecahedron) structure for Na_8.[27] The resulting di-

TABLE II. Optimized geometries for trimer and tetramer NaLi clusters and DFT calculated static dipole polarizability per atom (in Å^3), along the principal axes α_{ii}/n and corresponding average polarizability per atom (in Å^3), $\alpha_{moy}/n=1/3(\alpha_{xx}+\alpha_{yy}+\alpha_{zz})/n$. $\bar{r}$ is the average bond length. See Fig. 3 for the definitions of R_1, R_2, R_3, γ, and β. Calculated results for Na_8 and Li_8 are also given, as well as present experimental values.

	Sym.		$\bar{r}$ (Å)	R_1 (Å)	R_2 (Å)	R_3 (Å)	γ(°)	β(°)	α_{xx}/n	α_{yy}/n	α_{zz}/n	α_{moy}/n
Li_3	C_{2v}	DFT/PW91	2.98	2.82	2.82	3.30	71.6	54.2	10.3	25.2	14.2	16.6
		CISD(3*e*)[a]							10.4	25.4	12.7	16.1
		CISD(all *e*)[a]							10.6	25.9	11.7	16.1
		Exp.[b]		2.73	2.73	3.20	71.8	54.1				
		Exp.										11.5
Li_2Na	C_s	DFT/PW91	3.16	3.13	3.58	2.76	47.9	74.6	11.3	16.2	25.6	17.7
		Exp.										11.8
$LiNa_2$	C_{2v}	DFT/PW91	3.40	3.05	3.05	4.10	84.5	47.8	12.4	29.5	16.7	19.5
		Exp.										20.4
Na_3	C_{2v}	DFT/PW91	3.65	3.28	3.28	4.38	83.7	48.2	13.6	32.6	18.5	21.6
		Exp.										21.7
	Sym.		$\bar{r}$	R_1 (Å)	R_2 (Å)	R_3 (Å)	R_4 (Å)	γ(°)	β(°)	α_{xx}/n	α_{yy}/n	α_{zz}/n	α_{moy}/n
Li_4	C_{2v}	DFT	2.99	3.07	3.07	3.07	3.07	128.6	51.4	9.0	23.5	11.1	14.5
		Exp.											12.3
Li_3Na	C_{2v}	DFT	3.07	3.07	3.07	3.27	3.27	129.9	51.8	9.5	24.9	11.8	15.4
		Exp.											13.7
Li_2Na_2	C_{2v}	DFT	3.16	3.28	3.28	3.28	3.28	131.3	48.7	10.0	26.3	12.4	16.2
		Exp.											15.0
$LiNa_3$	C_{2v}	DFT	3.44	3.54	3.29	3.29	3.54	120.4	50.5	10.7	29.1	13.7	17.8
		Exp.											18.9
Na_4	C_{2v}	DFT	3.48	3.57	3.57	3.57	3.57	128.0	52.0	11.5	32.4	14.8	19.6
		Exp.											21.0
			$\bar{r}$ (Å)		α_{xx}/n		α_{yy}/n			α_{zz}/n			α_{moy}/n
Li_8		DFT	3.11		11.2		11.2			10.9			11.1
		Exp.											10.4
Na_8		DFT	3.58		14.1		14.1			16.4			14.9
		Exp.											16.8

[a]Calculations performed with the DFT/PW91 geometry.
[b]Reference 23.

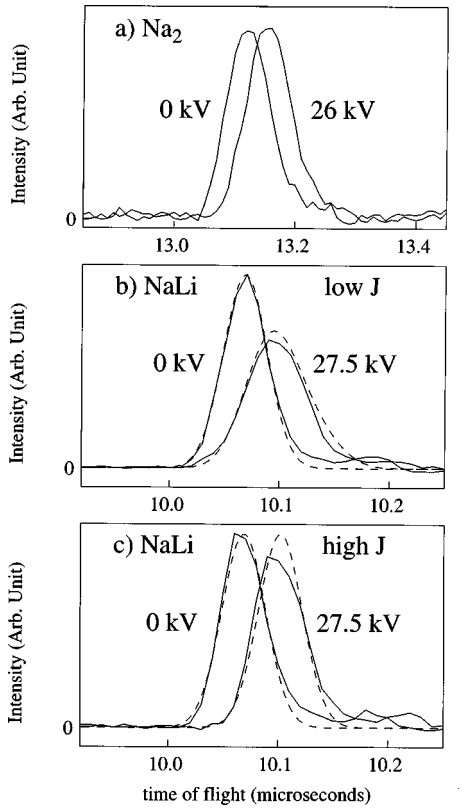

FIG. 4. Beam deflection profiles for Na_2 molecules (a), NaLi molecules ($J=4-6$) (b), and NaLi molecules ($J=12-14$) (c), with and without electric field in the deflector. The dashed lines represent the fitted curves obtained for $J=4$, 5, 6 (b), and $J=12$, 13, 14 (c), with $\alpha_s=39\,\text{Å}^3$ and $\mu=0.49$ D.

agonal components α_{xx}, α_{yy}, and α_{zz}, per atom and the average polarizability α_{moy} per atom for trimers, tetramers, Na_8, and Li_8 are given in Table II.

IV. DIATOMIC MOLECULES

A. Arrival time distributions (ATD's)

Diatomic molecules are ionized by resonant two-photon ionization spectroscopy. Figure 4(a) shows typical ATD profiles at the detector (TOF1), for the Na_2 molecule with and without electric field. In Fig. 4(a), the Na_2 $A\,^1\Sigma_u^+(v'=8) \leftarrow X\,^1\Sigma_g^+(v''=0)$ transition is excited by a dye laser at $\lambda=642.25$ nm (the resolution of the laser is about 0.4 cm^{-1}). The absorption corresponds typically to the R ($J''=9\rightarrow J'=10$) and the P ($J''=10\rightarrow J'=9$; $J''=11\rightarrow J'=10$) lines. A second photon ($\lambda=308$ nm) ionizes the excited molecules. The difference in arrival time for Na_2, with (26 kV) and without electric field is about 34 ns, which represents a deviation of the beam of a few tenths of a millimeter. The profiles of the ATD's and the deviation are not affected whatever the wavelength used for the excitation, and therefore whatever the selected J value. A similar behavior is obtained for Li_2 deflections. Figures 4(b) and 4(c) display the ATD's for the NaLi molecule. The NaLi $B\,^1\Pi(v'=7) \leftarrow X\,^1\Sigma(v''=0)$ transition is excited for two different positions in the rotation band. Figure 4(b) displays the ATD's when molecules are excited at $\lambda=475.6$ nm, which corresponds to a selection of molecules with ''low'' rotational angular momentum J ($J''=4$, 5, and 6). In Fig. 4(c), molecules with ''high'' rotational angular momentum J ($J''=12$, 13, and 14) are selected. Clearly, we see that the ATD's measured with the deflection field on NaLi are J dependent. Indeed, for molecules with low J levels, the distribution is broadened by the deviation field. For molecules with high J levels, the shapes of the profiles remain almost the same, the deflection with the applied field is stronger. This difference between Na_2, Li_2, and NaLi is due to the permanent dipole of NaLi.

B. Stark analysis

The Hamiltonian of a linear rigid rotator with a permanent dipole moment μ in an external field $\mathbf{F}$ is given by

$$H=H_{\text{rot}}+H_\mu+H_p=B\mathbf{J}^2-\mu\mathbf{F}-\frac{1}{2}\mathbf{F}\alpha\mathbf{F}, \tag{4}$$

where B is the rotational constant, $\mathbf{J}$ is the rotational angular momentum operator.

The energy corresponding to the Hamiltonian H is calculated by perturbation with $H_\mu+H_p$ as the perturbing term. In H_p, due to molecular symmetry, $\alpha_{xx}=\alpha_{yy}$, then,

$$H_p=-\frac{1}{2}[(\alpha_{zz}-\alpha_{xx})\cos^2\theta+\alpha_{xx}]F^2. \tag{5}$$

θ is the angle between the field direction and the molecular axis. The first-order energy correction is proportional to the second power of the field,

$$E_p=\langle JM|H_p|JM\rangle = -\frac{1}{2}\left[\alpha_s+\frac{2}{3}\alpha_a\left(\frac{J(J+1)-3M^2}{(2J+3)(2J-1)}\right)\right]F^2, \tag{6}$$

where $\alpha_a=\alpha_{zz}-\alpha_{xx}$ is the polarizability anisotropy and $\alpha_s=(1/3)(2\alpha_{xx}+\alpha_{zz})$ is the symmetric polarizability.

For the interaction energy due to the permanent dipole moment (H_μ), the first-order correction to the unperturbed energy levels is zero. It can be shown that the second-order correction has the form,[28]

$$E_\mu=\frac{\mu^2F^2}{2BJ(J+1)}\left\{\frac{J(J+1)-3M^2}{(2J-1)(2J+3)}\right\}. \tag{7}$$

E_p and E_μ are in the same order of magnitude, they are proportional to F^2. The second-order correction coming from H_p is much smaller. Thus, the net energy correction due to the permanent and induced dipole moment is

$$W=E_p+E_\mu=-\frac{1}{2}\alpha_{\text{eff}(JM)}F^2, \tag{8}$$

where $\alpha_{\text{eff}(JM)}$ is given by

$$\alpha_{\text{eff}(JM)}=\alpha_s-\left[\frac{J(J+1)-3M^2}{(2J-1)(2J+3)}\right]\left(\frac{\mu^2}{BJ(J+1)}-\frac{2}{3}\alpha_a\right). \tag{9}$$

If $\mu=0$ (Na_2 and Li_2), and if the contribution from α_a is neglected (which can be done for all the molecules that we have studied), the force $\mathbf{f}$ acting on molecules is given by

$-\alpha_s$**FgradF** and does not depend on the rotational level of the molecule. All the molecules are deviated by the same amount. If $\mu \neq 0$ (NaLi), the energy of the molecule and then the force depends on the quantum numbers J and M. The molecular beam is split by the electrical field and then the arrival time at the detector depends on the rotational level of the molecule. The values of the E_μ term decrease as J or the rotational temperature increases. At high J-levels, for molecules with small permanent dipole moment, and neglecting the second term in polarizability [α_a in Eq. (9)], the effective polarizability reduces to the average polarizability given by the symmetric polarizability. A deflection without broadening is obtained. We have also studied NaLi molecules by single-photon ionization. With a one-photon ionization process, all the J levels which are populated according to the Boltzmann law, are ionized. For a temperature T the term due to the permanent dipole moment, for the levels which are the most populated, varies like $(1-3\cos^2\theta)\mu^2/4kT$. For the source conditions that we are using, this term is weak as compared to the symmetric polarizability term (with high values of J preferentially populated). We observe a shift of the dispersion without broadening.

For diatomic molecules (and planar molecules), a very slight orientation of the molecules in the supersonic beam cannot be excluded. This would affect the measurement slightly. The measured value would not exactly correspond to the arithmetic average of the three diagonal elements of the polarizability tensor.

C. Polarizability and permanent dipole moment

For homonuclear diatomic molecules, polarizabilities are directly obtained from the time shift observed on the ATD's. The polarizability values α_s measured for the sodium and lithium dimers (40 and 32.8 Å^3, respectively) are in good agreement with recent published data (39 and 40 Å^3 for Na_2[7,29] and 34 Å^3 for Li_2[29]). As already mentioned in Sec. III, a good agreement between experimental and our DFT, as well as all-electrons CISD calculated polarizabilities, is obtained for the alkali dimers.

For NaLi molecules, the average polarizability and the permanent dipole have been obtained by fitting the arrival time distribution using the gradient of Eq. (8), $\mathbf{f} = -\alpha_{\text{eff}}$**FgradF**. For these simulations, we assumed a Gaussian profile for the distribution without deviation. The effect of the asymmetric polarizability term α_a is seen to be very small, and we used the calculated value 20.2 Å^3 in our simulations. Values for μ and α_s were fitted on a set of ATD's obtained for different J ($0 \leqslant J \leqslant 15$) and different voltages across the deviator. We found $\alpha_s = 39 \pm 3$ Å^3 and $\mu = 0.49 \pm 0.02$ D. The fit obtained for $J=4$, 5, and 6 and $J=12$, 13, and 14 ($V=27.5$ kV) are plotted in Figs. 4(b) and 4(c) (dashed lines). These data are in excellent agreement with previous published results given by a Stark analysis of the NaLi hyperfine structure ($\alpha_s = 40$ Å^3 and $\mu = 0.46$ D),[30] and with our *ab initio* calculated values ($\alpha_s = 35.4$ Å^3 and $\mu = 0.48$ D, see Table III).

TABLE III. Experimental static dipole polarizability per atom for $Na_{x-y}Li_y$ clusters. (Experimental errors are in the range of 4% for dimers and of 10% clusters.)

	α/n[Å^3]
Na_2	20.0
NaLi	19.5
Li_2	16.4
Na_3	21.7
Na_2Li	20.4
$NaLi_2$	11.8
Li_3	11.5
Na_4	21.0
Na_3Li	18.9
Na_2Li_2	15.0
$NaLi_3$	13.7
Li_4	12.3
Na_8	16.8
Na_6Li_2	19.2
Na_5Li_3	17.4
Na_4Li_4	16.5
Na_3Li_5	14.3
Na_2Li_6	14.6
$NaLi_7$	8.2
Li_8	10.4

V. NaLi CLUSTERS

A. Experimental results

Figure 5 shows the beam profiles of Na_2Li_2 and Na_3Li clusters with and without electric deflecting field. The clusters are ionized in a one-photon process (with the fourth

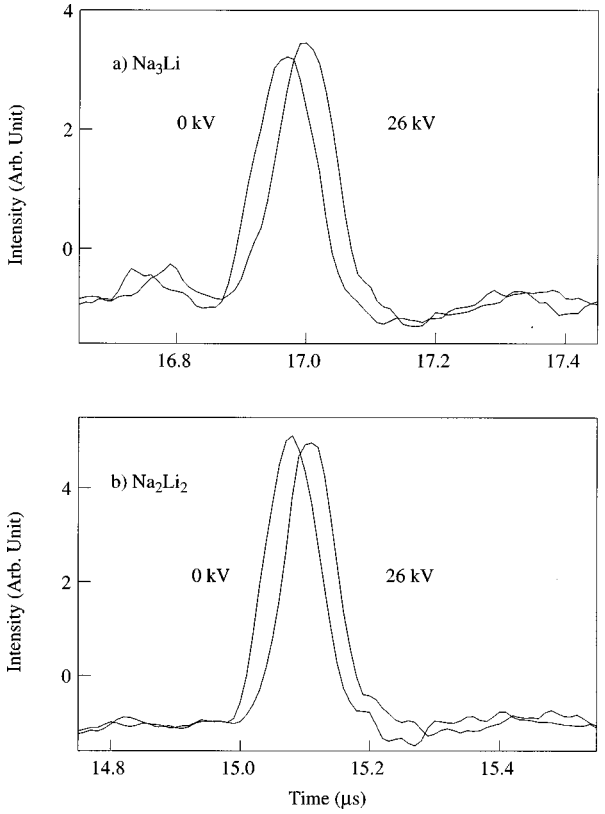

FIG. 5. Beam deflection profiles for Na_3Li (a) and Na_2Li_2 (b) clusters, with and without electric field in the deflector (0 and 26 kV).

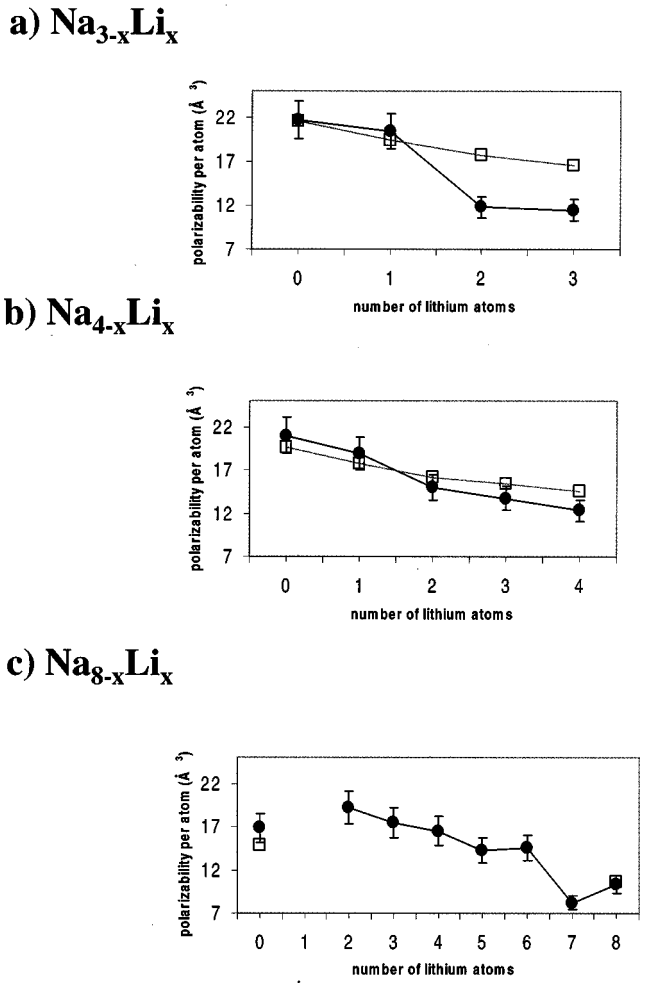

FIG. 6. Experimental (●) and DFT calculated (□) static dipole polarizabilities per atom for the $Na_{y-x}Li_x$ clusters (with $y=3$, 4, and 8).

harmonic of a Nd:YAG), thus the experimentally observed effective polarizability is an average over rotational and vibrational state distributions. We want to emphasize that in our experiment, the ATD profiles of both pure alkali clusters and NaLi clusters present no broadening. This may look surprising since asymmetric heterogeneous clusters are predicted to possess a permanent dipole moment. These mixed sodium–lithium clusters are asymmetric top rotors. First order of the Stark effect of zero.[28] The second order of the Stark effect is proportional to $1/kT$. Under the clustering source conditions, the temperature extracted from evaporative ensemble experiments on neutral sodium clusters has been found to be about 400 K.[31] Clusters are ionized by a one-photon process, the signal is mainly due to clusters with high values of J, and this second-order term can be neglected as experimentally observed.

Figure 6 shows the absolute static polarizability (per atom) for small heterogeneous $Na_{y-x}Li_x$ clusters, for systems with $y=3$, 4, and 8. The experimental values are listed in Table III. For the alkali clusters, the polarizability of small lithium clusters is significantly lower than those for sodium clusters. The mean trend in the polarizability of heterogeneous $Na_{y-x}Li_x$ clusters, for a given y number of valence electrons, is a continuous decrease of α with the increase in lithium content. A strong fall of the polarizability between Na_2Li and $NaLi_2$ is observed in the trimer series, whereas for tetramer and octamer series, a smoother decrease of the polarizabilities is observed.

TABLE IV. Comparison of static dipole polarizability (in Å^3) per atom with different theoretical estimates.

	Theory	α_{xx}/n	α_{yy}/n	α_{zz}/n	α_{moy}/n
Li_4	This work	9.0	23.5	11.1	14.5
	Ref. 25	8.1	20.3	10.7	13.0
Li_3Na	This work	9.5	24.9	11.8	15.4
	Ref. 25	9.4	23.6	11.7	14.9
Li_2Na_2	This work	10.0	26.3	12.4	16.2
	Ref. 25	10.5	27.2	12.7	16.8
$LiNa_3$	This work	10.7	29.1	13.7	17.8
	Ref. 25	11.5	29.7	14.3	18.5
Na_4	This work	11.5	32.4	14.8	19.6
	Ref. 25	12.5	32.7	16.0	20.4
	Ref. 33	20.3	34.0	15.0	23.1
	Theory	α_{xx}/n	α_{yy}/n	α_{zz}/n	α_{moy}/n
Li_8	This work	11.2	11.2	10.9	11.1
	S.O.S.[a,b]	10.4	10.4	10.4	10.4
	TDLDA[c]				10.3
Na_8	This work	14.1	14.1	16.4	14.9
	S.O.S.[a,b]	16.5	16.5	16.5	16.5
	TDLDA[c]				14.3[e]
	TDLDA[c]				15.4[e]
	LSDA[d]	15.0	15.0	15.0	15.0

[a]Sum over states calculation using calculated oscillator strengths from nonlocal pseudopotentials.
[b]Reference 8.
[c]Reference 32.
[d]Reference 33.
[e]Corresponds to two different pseudopotentials.

B. Comparison with *ab initio* calculations

The average polarizabilities determined by DFT calculations are also plotted in Fig. 6. The overall agreement is good. Main trends are well reproduced. Except for $NaLi_2$ and Li_3, calculated values are within the error bars. For trimers, *ab initio* calculations (DFT and all-electrons CISD for Li_3, see Table II) are not able to reproduce the sharp decrease in polarizability observed between Na_2Li and $NaLi_2$. This discrepancy is not fully understood. For tetramers, a good agreement is obtained. Our calculated values are also very close to previous Hartree–Fock (HF) *ab initio* calculations of Dahlseid *et al.*[25] (see Table IV). For octamers, *ab initio* polarizability calculations have been performed only for Na_8 and Li_8. A very good agreement, both for Na_8 and Li_8, is obtained with experimental polarizabilities. As seen in Table IV, a similar agreement is observed with other reported calculations of the static polarizability of alkali octamers within the framework of the time-dependent local density approximation (TDLDA) [$\alpha(Na_8)=123.2$, $\alpha(Li_8)=82.7$ Å^3],[32] self-consistent local-spin-density approximation (SCLSDA) calculations [$\alpha(Na_8)=120.0$ Å^3],[33] and sum over states calculations using calculated oscillator strengths from nonlocal pseudopotentials [$\alpha(Na_8)=118.4$, $\alpha(Li_8)=84.7$ Å^3].[8]

The static response to an electric field can be compared to the dynamic response to an electromagnetic wave field.

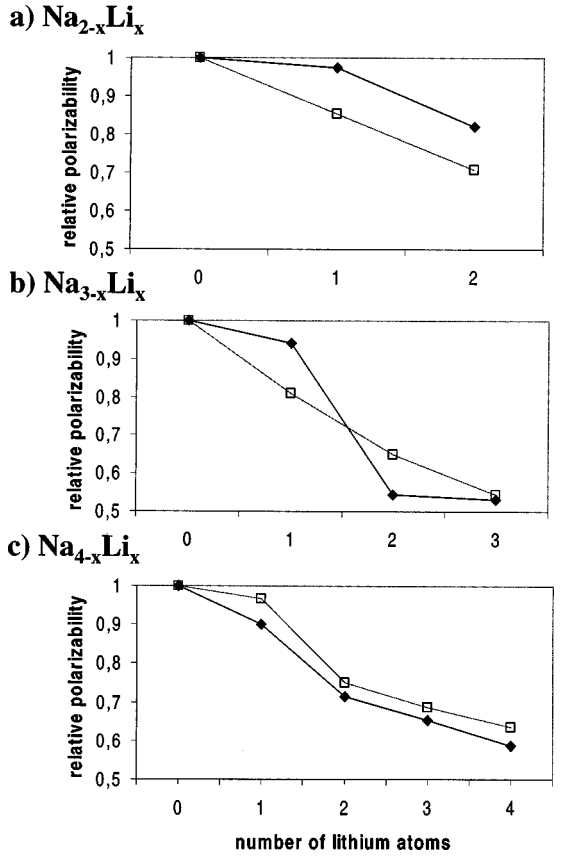

FIG. 7. Experimental polarizability of mixed clusters relative to pure sodium cluster polarizability $\alpha/\alpha_{\mathrm{Na}_n}$ (◆), and calculated relative average bond length to the power 3 $(\overline{r/r}_{\mathrm{Na}_n})^3$ (□).

For a finite metallic sphere, the classical Mie–Drude theory relates the static polarizabilities and the surface plasmon frequencies,

$$\omega_{0i}^2=\frac{Ne^2}{m\alpha_{ii}}, \tag{10}$$

where N is the number of valence electrons, m and e are, respectively, the mass and the charge of the electron. In lithium clusters, as recently experimentally probed by Benichou *et al.*,[8] due to nonlocal electron ion interactions, the oscillator strength in the visible part of the spectrum is reduced. In Eq. (10), N should be replaced by N_{eff}. Blundell and Guet predicted a value per valence electron of 0.77 for lithium.[34] For Na_4, plasmon frequencies ($\lambda_x=401.2$, $\lambda_z=455.2$, $\lambda_y=673.5$ nm) obtained with formula (10) and our calculated polarizabilities are in good qualitative agreement with experimental absorption spectra measured by Wang *et al.* (440, 495, 690 nm).[35] For lithium clusters and using $N_{\mathrm{eff}}=0.77$ per atom, we obtained a similar agreement ($\lambda_x=444.9$, $\lambda_z=494.1$, $\lambda_y=718.9$ nm) with the absorption spectra (430, 470, 690 nm).[36] Note that in this case, a calculation without the oscillator strength reduction leads to a strong overestimation of absorption frequencies. Similar agreements are obtained for Na_8 ($\lambda\cong 492$ nm)[37,38] and Li_8 ($\lambda\cong 477$ nm).[39] For mixed $Na_{4-x}Li_x$ clusters, following Pollack *et al.*,[40] one can use $N_{\mathrm{eff}}=xN_{\mathrm{eff}}^{\mathrm{Li}}/4+(4-x)N_{\mathrm{eff}}^{\mathrm{Na}}/4$ per atom. Frequencies obtained with these oscillator strengths are in agreement with depletion spectra.[40] The comparison of our experimental polarizabilities with absorption spectra is a proof that the oscillator strength is reduced in mixed sodium–lithium clusters.

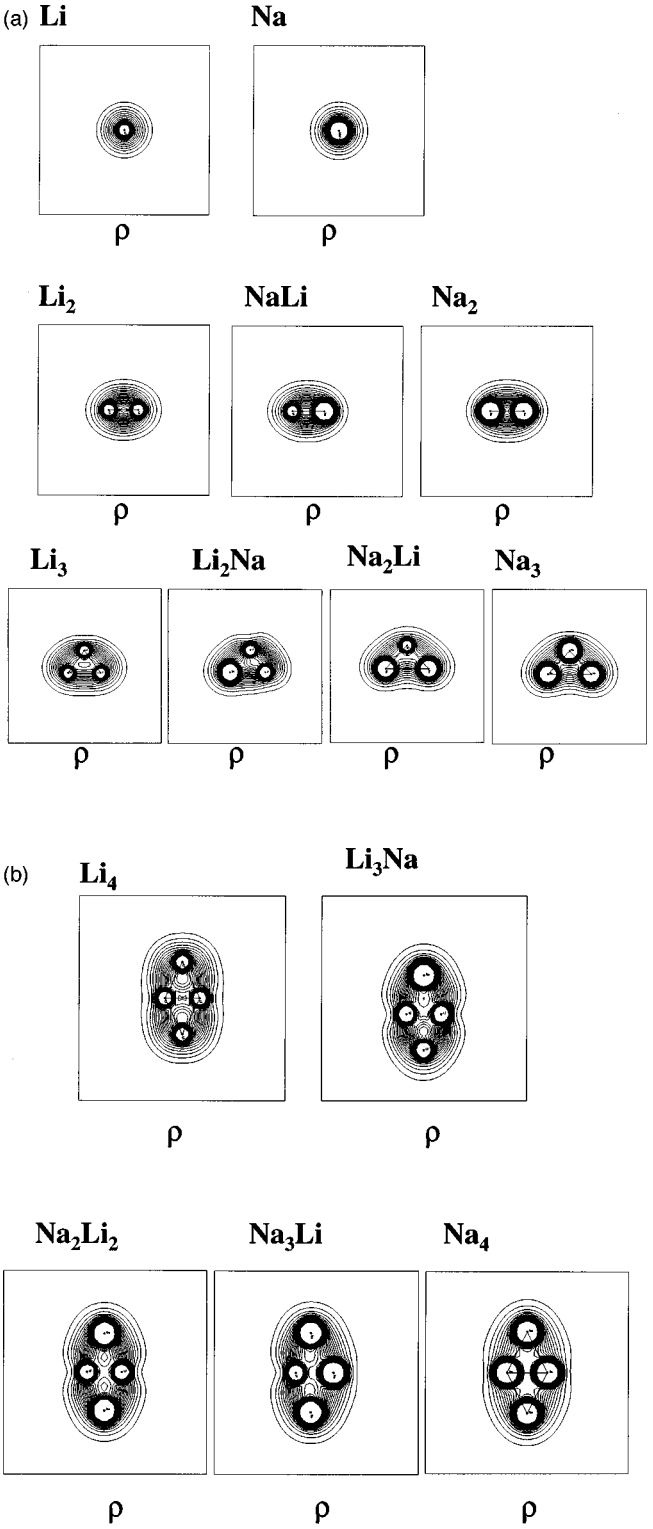

FIG. 8. (a) Electronic densities ρ for the $Na_{y-x}Li_x$ clusters with $x=1$, 2, 3. The outer isodensity contour corresponds to 5.10^{-4} for each cluster. (b) Electronic densities ρ for the $Na_{y-x}Li_x$ clusters with $x=4$. The outer isodensity contour corresponds to 5.10^{-4} for each cluster.

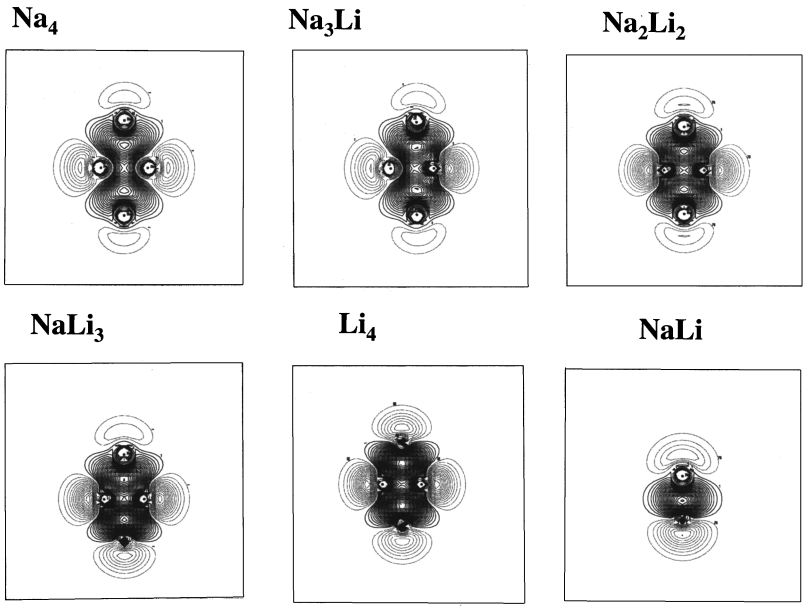

FIG. 9. Differential electronic densities $\delta\rho=\rho-\rho$ (atoms) for the Li_4, Li_3Na, Li_2Na_2, $LiNa_3$, Na_4, and NaLi molecules. The values of positive contours are labeled by solid lines, while negative values are labeled by dashed lines. The outer isodensity contour corresponds to 2.10^{-4} for each cluster.

C. Discussion

Na–Li and Li–Li bonds are stronger and shorter than Na–Na bonds. A large part of the decrease in polarizability observed from Na_n to Li_n clusters is due to the decrease in bond length. This decrease induces an increase of the valence electron density in the cluster. In the bulk limit, the polarizability of a lithium sphere ($\alpha=R^3$) is 46% lower than the polarizability of a sodium sphere, since sodium and lithium Wigner–Seitz radii are 2.12 and 1.75 Å, respectively. The ratios observed for tetramers and octamers [$\alpha(Li_4)/\alpha(Na_4)=0.59$ and $\alpha(Li_8)/\alpha(Na_8)=0.61$] are close to the bulk limit ratio ($\sim$0.54). In Fig. 7 we have plotted the evolution of the experimental polarizabilities as compared to the evolution of the calculated average bond length to the power 3 in mixed sodium–lithium clusters. Values of the polarizability and of the length to the power 3 are divided by pure sodium clusters' values. For the size 3, a good qualitative agreement is observed, although the strong diminution in the polarizability between Na_2Li and $NaLi_2$ is not reproduced by the bond length evolution. For sizes 4 and 8, the evolution of the polarizability and bond length to the power 3 are very similar. For these sizes, the polarizability depends mainly on the volume of the cluster as expected for a small metallic droplet.[11,41]

Different trends are observed for size 2. For dimers, the difference in polarizability from pure sodium molecules to pure lithium molecules is much smaller than the one expected from the bond length evolution. The relatively large polarizability of very small lithium-rich clusters is related to the high polarizability of lithium atom. In a classical model, the polarizability depends on the size of the electronic cloud. Total electronic density ρ for mixed NaLi clusters from monomers to tetramers is plotted in Figs. 8(a) and 8(b). The outer isodensity contour corresponds to $5\cdot10^{-4}$. The volumes encapsulating non-negligible electronic density for sodium and lithium atoms are very similar, although electronic density due to core electrons is very different. This explains the similarity of sodium and lithium atom polarizability. For dimers, bond lengths and electronic density are different. Moreover, the volume occupied by valence electrons is almost equal in Na_2, NaLi, and Li_2. Due to a higher diffusion of valence electrons in dimers, which contain a Li atom, a very slow decrease in polarizability is observed from Na_2 to Li_2.

For trimers and tetramers, these figures show that the valence electrons are not localized on the ionic core or between two atoms, but are delocalized between the different atoms. The bonding between the atoms is due to a transfer of electrons from the outside to the inside of the cluster. The delocalization of the valence electrons between the atoms is a precursor of the metallic bonding in these clusters. The bond lengths of lithium-rich clusters are smaller than those of sodium-rich clusters. There is also a slight reduction of the size of the electronic cloud from sodium-rich to lithium-rich clusters. In particular, valence electrons are less diffuse in lithium clusters than in lithium atom or NaLi and Li_2 molecules. This effect is less pronounced in sodium clusters. Figure 9 displays the differential density $\delta\rho=\rho-\rho$ (atoms) for mixed tetramers. A stronger electron transfer from the atoms to the inside of the cluster is observed for Li_4 than for Na_4. In a mixed cluster, the participation to the bonding of Li valence electrons is higher than the participation of the Na valence electrons. The lithium valence electron, which is very diffuse in the Li atom, is quickly driven in the cluster to form a strong bonding. The very diffuse character of the Li valence orbital disappears in clusters for sizes as small as 3–4. This contraction of the electronic cloud is characterized by the decrease in the polarizability of lithium-rich clusters, and corresponds to the onset of delocalized electrons in these clusters.

Finally, as also displayed in Fig. 9, the differential electron density map for the NaLi molecule shows that, already for this size, the electron transfer to form the bonding is

higher for Li than for Na, which induces the permanent dipole that we have measured and calculated.

VI. CONCLUSION

We have measured the static dipole polarizability of $Na_{y-x}Li_x$ clusters (with $y=2$, 3, 4, and 8) by the molecular beam deflection technique. For diatomic molecules, experimental polarizabilities are in good agreement with both previous experimental data and our *ab initio* calculated polarizabilities. Furthermore, for the NaLi molecule, both permanent dipole and average polarizability have been obtained. For mixed clusters, polarizabilities are found to decrease continuously from pure sodium to pure lithium clusters, as a function of the lithium content. Experimental polarizabilities are in good agreement with calculated values. For the dimer, the diffuse character of the atomic orbital in lithium remains important and explains the relatively high polarizability of NaLi. For trimers and tetramers, the onset of the metallic bonding dominates and tends to rub out the importance of the diffuse orbital of the lithium atom.

[1] W. A. de Heer, Rev. Mod. Phys. **65**, 631 (1993).
[2] M. Broyer and Ph. Dugourd, Comments At. Mol. Phys. **31**, 183 (1995).
[3] V. Bonacic-Koutecky, C. Fuchs, J. Pittner, L. Cespiva, P. Fantucci, and J. Koutecky, Comments At. Mol. Phys. **31**, 233 (1995).
[4] E. Benichou, A. R. Allouche, M. Aubert-Frécon, R. Antoine, M. Broyer, Ph. Dugourd, and D. Rayane, Chem. Phys. Lett. **290**, 170 (1998).
[5] T. M. Miller and B. Bederson, Adv. At., Mol., Opt. Phys. **25**, 37 (1998).
[6] J. K. Nagle, J. Am. Chem. Soc. **112**, 4741 (1990).
[7] W. D. Knight, K. Clemenger, W. A. de Heer, and W. A. Saunders, Phys. Rev. B **31**, 2539 (1985).
[8] E. Benichou, R. Antoine, D. Rayane, B. Vezin, F. W. Dalby, Ph. Dugourd, M. Broyer, Ch. Ristori, F. Chandezon, B. A. Huber, J. C. Rocco, S. A. Blundell, and C. Guet, Phys. Rev. A **59**, R1 (in press).
[9] N. F. Ramsay, *Molecular Beams* (Oxford University Press, Oxford, 1969).
[10] W. A. de Heer and P. Milani, Rev. Sci. Instrum. **62**, 670 (1991).
[11] K. D. Bonin and V. V. Kresin, *Electric-Dipole Polarizabilities of Atoms, Molecules and Clusters* (World Scientific, Singapore, 1997).
[12] A. H. Shapiro, *The Dynamics and Thermodynamics of Compressible Fluid Flow* (Ronald, New York, 1953).
[13] J. P. Perdew and Y. Wang, Phys. Rev. B **45**, 13,244 (1992).
[14] A. J. Sadlej and M. Urban, J. Mol. Struct.: THEOCHEM **80**, 234 (1991).
[15] D. Rayane, A.-R. Allouche, E. Benichou, R. Antoine, M. Aubert-Frécon, Ph. Dugourd, M. Broyer, C. Ristori, F. Chandezon, B. A. Huber, and C. Guet, Eur. Phys. J. D (in press).
[16] B. G. Johnson and M. J. Fisch, J. Chem. Phys. **100**, 7429 (1994).
[17] GAUSSIAN 94, revision B.3, M. F. Frisch, G. W. Trucks, H. B. Schlegel, P. M. W. Gill, B. G. Johnson, M. A. Robb, J. R. Cheeseman, T. Keith, G. A. Petersson, J. A. Montgomery, K. Raghavachari, M. A. Al-Laham, V. G. Zakrzewski, J. V. Ortiz, J. B. Foresman, C. Y. Peng, P. Y. Ayala, W. Chen, M. W. Wong, J. L. Andres, E. S. Replogle, R. Gomperts, R. L. Martin, D. J. Fox, J. S. Binkley, D. J. Defrees, J. Baker, J. P. Stewart, M. Head-Gordon, C. Gonzalez, and J. A. Pople (Gaussian, Inc., Pittsburgh, PA, 1995).
[18] K. Andersson, M. R. A. Blomberg, M. P. Fülsher, V. Kellö, R. Lindh, P. A. Malmqvist, J. Noga, J. Olsen, B. O. Roos, A. J. Sadlej, P. E. M. Siegbahn, M. Urban, and P. O. Widmark, MOLCAS, Version 2, University of Lund, Sweden.
[19] K. P. Huber and G. Hetzberg, *Molecular Spectra and Molecular Structure, Constants of Diatomic Molecules* (Van Nostrand Reinhold, New York, 1979).
[20] F. Engelke, G. Ennen, and M. Meiwes, Chem. Phys. **66**, 391 (1982).
[21] V. Bonacic-Koutecky, J. Gaus, M. F. Guest, L. Cespiva, and J. Koutecky, Chem. Phys. Lett. **206**, 528 (1993).
[22] I. Boustani, W. Pewestorf, P. Fantucci, V. Bonacic-Koutecky, and J. Koutecky, Phys. Rev. B **35**, 9437 (1987).
[23] Ph. Dugourd, J. Chevaleyre, M. Broyer, J.-P. Wolf, and L. Wöste, Chem. Phys. Lett. **175**, 555 (1990).
[24] D. Pavolini and F. Spiegelmann, J. Chem. Phys. **87**, 2854 (1987).
[25] T. A. Dahlseid, M. M. Kappes, J. A. Pople, and M. A. Ratner, J. Chem. Phys. **96**, 4924 (1992).
[26] V. Bonacic-Koutecky, J. Gaus, M. F. Guest, and J. Koutecky, J. Chem. Phys. **96**, 4934 (1992).
[27] M-W. Sung, R. Kawai, and J. H. Weare, Phys. Rev. Lett. **73**, 3552 (1994).
[28] C. H. Townes and A. L. Schawlow, *Microwave Spectroscopy* (Mc Graw-Hill, New York, 1955).
[29] V. Tarnovsky, M. Bunimovicz, L. Vuskovic, B. Stumpf, and B. Bederson, J. Chem. Phys. **98**, 3894 (1993).
[30] J. Graff, P. J. Dagdigian, and L. Wharton, J. Chem. Phys. **57**, 710 (1972).
[31] Ph. Dugourd, D. Rayane, R. Antoine, and M. Broyer, Chem. Phys. **218**, 163 (1997).
[32] J. M. Pacheco and J. L. Martins, J. Chem. Phys. **106**, 6039 (1997).
[33] I. Moullet, J. L. Martins, F. Reuse, and J. Buttet, Phys. Rev. Lett. **65**, 476 (1990).
[34] S. A. Blundell and C. Guet, Z. Phys. D **33**, 153 (1995).
[35] C. R. C. Wang, S. Pollack, D. Cameron, and M. M. Kappes, J. Chem. Phys. **93**, 3787 (1990).
[36] M. Broyer, J. Chevaleyre, Ph. Dugourd, J.-P. Wolf, and L. Wöste, Phys. Rev. A **42**, 6954 (1990).
[37] K. Selby, M. Vollmer, J. Masui, V. Kresin, W. A. DeHeer, and W. D. Knight, Phys. Rev. B **40**, 5417 (1989).
[38] C. R. C. Wang, S. Pollack, and M. Kappes, Chem. Phys. Lett. **166**, 26 (1990).
[39] J. Blanc, V. Bonacic-Koutecky, M. Broyer, J. Chevaleyre, Ph. Dugourd, J. Koutecky, C. Scheuch, J. P. Wolf, and L. Wöste, J. Chem. Phys. **96**, 1783 (1992).
[40] S. Pollack, C. R. C. Wang, T. A. Dahlseid, and M. M. Kappes, J. Chem. Phys. **96**, 4918 (1992).
[41] C. Kittel, *Introduction to Solid State Physics* (Wiley, New York, 1976).